Non-Markovianity and a generalized Landauer bound for a minimal quantum autonomous thermal machine with a work qubit

A. Khoudiri[1,*] A. El Allati[1,2,†] ÖE. Müstecaplıoğlu[3,4,5,‡] and K. El Anouz[1,§]
[1]*Laboratory of R&D in Engineering Sciences, Faculty of Sciences and Techniques Al-Hoceima, Abdelmalek Essaadi University, Tetouan, Morocco*
[2]*Max Planck Institute for the Physics of Complex Systems, Nöthnitzer Str. 38, D-01187 Dresden, Germany*
[3]*Department of Physics, Koç University, Istanbul, Sarıyer 34450, Türkiye*
[4]*TÜBİTAK Research Institute for Fundamental Sciences, 41470 Gebze, Türkiye*
[5]*Faculty of Engineering and Natural Sciences, Sabancı University, Tuzla 34956, Türkiye*

(Received 25 August 2024; revised 29 January 2025; accepted 13 March 2025; published 16 April 2025)

We investigate the validity of the Landauer principle in the context of a non-Markovian environment, employing a quantum autonomous thermal machine (QATM) comprised of two qubits, attached to different Markovian thermal reservoirs coupled to a single qubit acting as a quantum coherence reservoir, interpreted as a working qubit. We numerically demonstrate that the non-Markovianity, arising from the exchange of correlations between the QATM qubits and the work qubit, influences the Landauer bound. We analyze two distinct reservoir types: fermionic and bosonic, and show that the QATM, operating as a single entity, interacts with the work qubit at an effective virtual temperature, leading to a violation of the conventional Landauer bound. Consequently, we derive a lower bound for the minimal dissipation energy required to erase information during the energy exchange between the QATM and the work qubit. The QATM's information engine character and impact on the work qubit is further characterized by monitoring its information content, including coherence and population dynamics. Our analysis reveals that the work qubit's populations oscillate in time, while the coherence dissipates nonmonotonically.

DOI: 10.1103/PhysRevE.111.044124

I. INTRODUCTION

Quantum autonomous thermal machines (QATMs) have attracted much attention for investigating fundamental problems in quantum thermodynamics and making quantum technologies less reliant on external control [1–4]. In addition to more conventional studies, such as quantum Brownian autonomous heat engines and refrigerators [5–8], QATMs have been studied from the perspective of quantum information thermodynamics as well, including quantum entanglement generators [9–11] and energetic coherence managers [12]. In machine learning, QATMs are proposed to optimize finite-time thermodynamic processes [13]. Heat engines with quantum systems subject to external control have been realized with a single-ion [14], nitrogen-vacancy center [15], and spin systems [16,17]; and promising routes to realize QATM's experimentally have been proposed recently, too [18]. Another critical aspect explored is the impact of non-Markovian thermal operations on the performance of these machines, where non-Markovianity has been shown to enhance the efficiency of Otto engines and refrigeration cycles [8,9,19–21].

In the context of open quantum systems, one cannot always describe the dynamics of the open quantum systems using Markov approximation [22]. In general, the interaction between the open system and its environment for a time scale gives rise to more information loss about the memory effect of the open system evolution. It has been shown that one can study the evolution of an open quantum system using many techniques. Among them: are the Lindblad master equation [23], Heisenberg evolution, pseudomod evolution, and also stochastic methods [22]. Moreover, the non-Markovian dynamics can be created according to an ancillary qubit that filters the interaction of the open system with its surroundings to describe a structured non-Markovian environment strongly coupled to the system. In this inspiration, the memory effect is based on the correlations exchanged between the ancilla and the open system [24]. This paves the way for extending these concepts into the thermodynamic framework; including the effect of entropy exchange between the system and its environment, the relationship between the second law of thermodynamics and the concepts of Maxwell's demon to increase the control of the open quantum system [25]. This boosts the energy limits, fluctuations and non-Markovianity, to understand the fluctuations and the entropy production in a nanometer scale in the presence of multiple baths coupled to

*Contact author: khoudiri.achraf@etu.uae.ac.ma
†Contact author: eabderrahim@uae.ac.ma
‡Contact author: omustecap@ku.edu.tr
§Contact author: kelanouz@uae.ac.ma

an open system via auxiliary qubits [26]. Importantly, it has been highlighted that non-Markovianity plays an important role in the evolution of quantum thermal machines by analyzing the Otto and Carnot cycles [27].

Non-Markovianity in open quantum systems is generally attributed to memory effects in the system-environment interactions [28], characterized by the backflow of information from the environment to the system [29]. Particularly, the connection between thermodynamics and non-Markovian dynamics has been investigated. Indeed, the entropy production in non-Markovian quantum systems using the mesoscopic leads approach, as well as entropy production in strongly coupled systems with a Markovian embedding have been investigated [30]. Furthermore, the quantum Landauer principle [31] emerges from the intersection of thermodynamics and information theory, traditionally defining the minimum energy dissipation required to erase one bit of information through an irreversible transformation. The quantum Landauer bound extends this concept to the realm of quantum information erasure and thermodynamics [32]. Some studies have focused on how non-Markovian dynamics influence the Landauer limit [33–35]. While a QATM operates without external intervention, relying solely on its subsystems [1], it must be connected to a work or information reservoir for its usefulness. This raises several pertinent questions: How does non-Markovianity affect the dynamics of a QATM in the presence of an information reservoir? What is the relationship between the Landauer principle and non-Markovianity in the context of producing quantum coherence in a working qubit? How do quantum correlations in the system of QATM-work qubit and non-Markovianity influence the violation of the Landauer principle?

To address these questions, we propose a model of a QATM with a pair of qubits attached to their Markovian thermal reservoirs and both are coupled to a work qubit for storing quantum coherence. Our model relies on the exchange of excitations between machine qubits and the work qubit [36]. We consider two types of reservoirs: bosonic and fermionic [37,38]. Specifically, the time evolution of each qubit can be determined by solving the quantum master equation, which is based on the probabilistic interaction of the reservoirs with the machine-work qubit total system [39–41]. The pair of qubits of the QATM and their reservoirs can be envisioned as a single virtual machine qubit in contact with a single composite thermal bath of virtual qubits at a virtual temperature [47]. We shall use this interpretation to give physical insight into some of our results. The impact of QATM parameters on non-Markovianity is quantified using the trace distance [45], where nonmonotonic variations over time indicate non-Markovian dynamics, highlighting the prominence of memory effects. Our results suggest that the effect of QATM on the dynamics of the work qubit is more pronounced in fermionic than in bosonic reservoirs. To elucidate the backflow of information, we analyze correlations between the QATM and the work qubit using quantum mutual information [46], demonstrating that these correlations enhance information flow between the QATM and the work qubit. We find that the non-Markovian effect can violate the traditional Landauer bound, but a new, lower Landauer bound is confirmed across both Markovian and non-Markovian regimes.

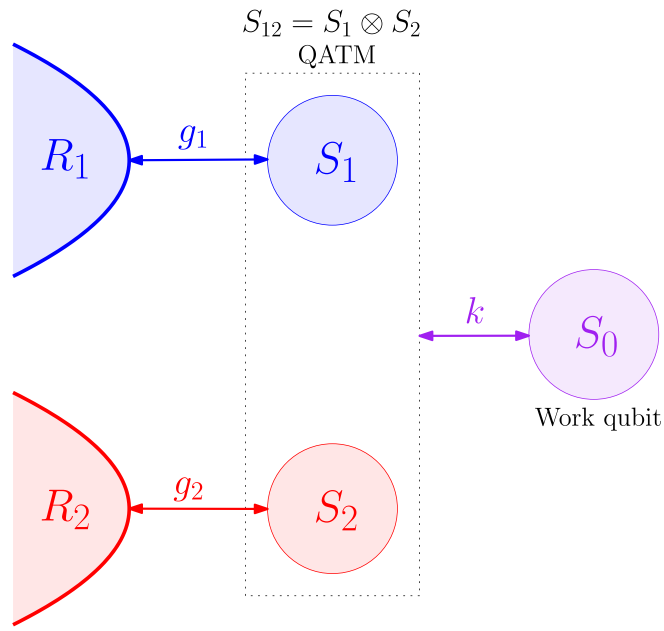

FIG. 1. Diagram of the two-qubit QATM S_1S_2 interacts with a working qubit S_0 that stores the quantum coherence produced by the machine. Moreover, the qubits S_1 and S_2 are attached to the Markovian reservoirs, namely R_1 and R_2, respectively. In contrast, the work qubit S_0 remains isolated from the environment and interacts directly with the QATM qubits via a coupling strength k. However, the interaction between qubit S_1 (S_2) and reservoirs R_1 (R_2) modes is governed via the coupling strengths g_1 (g_2).

The rest of the paper is structured as follows. In Sec. II, we introduced our theoretical model, where the Hamiltonian of the QATM-work qubit, i.e., the open system, including the master equation describing this open quantum system dynamics of the total system is presented. In Sec. III, we discuss our results, where we covered the QATM operation and work qubit dynamics in Sec. III A. In Sec. III B, we address the question of non-Markovianity and information exchange between the open system and the QATM, in terms of trace distance and mutual information analysis in Secs. III B 1 and III B 2, respectively. Section III C includes our findings on the relationship between the Landauer bound and non-Markovianity within the proposed autonomous quantum thermal machine. A conclusion is given in Sec. IV.

II. QATM-WORK QUBIT MODEL

We consider a total system, denoted by $T = S_1 \otimes S_2 \otimes S_0$, composed of three two-level systems (qubits), labeled S_0, S_1, and S_2. In this model, S_0 is isolated from the environment via the two qubits S_1 and S_2, where each of them is coupled to two Markovian reservoirs, R_1 and R_2, respectively, (see Fig. 1). Moreover, the composite system $S_{12} = S_1 \otimes S_2$ denotes the QATM, which generates and stores quantum coherence in S_0, referred to as the work qubit—a concept that will be further discussed in subsequent sections.

Model Hamiltonian and the master equation for QATM-work qubit system

The total Hamiltonian of our model, denoted by $\hat{H}$, is given by

$$\hat{H} = \hat{H}_T + \sum_{m=1}^{2} \hat{H}_{R_m} + \hat{H}_{S_{12}R}, \tag{1}$$

where

$$\hat{H}_T = \sum_{i=0}^{2} \hat{H}_{S_i} + \hat{H}_{S_{12}S_0} \tag{2}$$

is the Hamiltonian of the total qubit system T, where ($\hbar = 1$),

$$\hat{H}_{S_i} = E_{S_i} \hat{\sigma}^+_{S_i} \hat{\sigma}^-_{S_i}, \tag{3}$$

is the free Hamiltonian of the qubit S_i with energy gap E_{S_i}, where $i \in \{0, 1, 2\}$. We assume that $E_{S_2} = E_{S_1} + E_{S_0}$. Here, $\sigma^+_{S_i} = (\sigma^-_{S_i})^\dagger = |1_{S_i}\rangle \langle 0_{S_i}|$, where the operators act as $\sigma^+_{S_i} |0_{S_i}\rangle = |1_{S_i}\rangle$ and $\sigma^-_{S_i} |1_{S_i}\rangle = |0_{S_i}\rangle$. The states $|0_{S_i}\rangle$ and $|1_{S_i}\rangle$ represent the ground and excited states, respectively, of the qubit S_i, with $i \in \{0, 1, 2\}$.

The term $\hat{H}_{S_{12}S_0}$ represents the interaction Hamiltonian among the qubits. It is given by [12,36]

$$\begin{aligned}\hat{H}_{S_{12}S_0} = k\big(&\big|1_{S_1} 0_{S_2} 1_{S_0}\big\rangle\big\langle 0_{S_1} 1_{S_2} 0_{S_0}\big| \\ &+ \big|0_{S_1} 1_{S_2} 0_{S_0}\big\rangle\big\langle 1_{S_1} 0_{S_2} 1_{S_0}\big| \big),\end{aligned} \tag{4}$$

where k is the coupling coefficient between systems S_{12} and S_0. This interaction describes a minimal QATM [36], representing the excitation exchange among S_1, S_2, and S_0. Physically, the Hamiltonian in Eq. (4) drives the transition from $|0_{S_1} 1_{S_2} 0_{S_0}\rangle$ to $|1_{S_1} 0_{S_2} 1_{S_0}\rangle$ and its reverse, from $|1_{S_1} 0_{S_2} 1_{S_0}\rangle$ to $|0_{S_1} 1_{S_2} 0_{S_0}\rangle$. The transition from $|0_{S_1} 1_{S_2} 0_{S_0}\rangle$ to $|1_{S_1} 0_{S_2} 1_{S_0}\rangle$ corresponds to an increased probability of the excited states for systems S_1 and S_0, accompanied by a decreased probability of the excited state for system S_2. This indicates that the heat is transferred from qubit S_2 to qubit S_1 via S_0. Conversely, the transition from $|1_{S_1} 0_{S_2} 1_{S_0}\rangle$ to $|0_{S_1} 1_{S_2} 0_{S_0}\rangle$ represents the heat transfer from qubit S_1 to qubit S_2 through S_0. As we will see in the next sections, during these heat transfers, the populations of the work qubit S_0 evolve in oscillatory patterns over time, where quantum coherence is generated and temporarily stored in qubit S_0. Indeed, this can be interpreted as a result of the operation of the QATM [36].

The reservoirs are modeled as large ensembles of quantum harmonic oscillators, which can be either bosonic or fermionic, described by the free Hamiltonians

$$\hat{H}_{R_m} = \sum_k E_{mk} \hat{a}^\dagger_{mk} \hat{a}_{mk}, \tag{5}$$

where $\hat{a}_{mk}$ and $\hat{a}^\dagger_{mk}$ are the annihilation and creation operators of the reservoir modes, respectively, obeying bosonic or fermionic commutation relations. Each reservoir R_m is assumed to be in a thermal Gibbs state represented by the density matrix

$$\hat{\rho}_{R_m} = \frac{1}{Z_{R_m}} \mathrm{e}^{-\beta_{R_m} \hat{H}_{R_m}}, \tag{6}$$

where $Z_{R_m} = \mathrm{Tr}_{R_m}[\exp(-\beta_{R_m} \hat{H}_{R_m})]$ is the partition function, and $\beta_{R_m} = 1/T_m$ ($m \in \{1, 2\}$) is the inverse temperature (with the Boltzmann constant $k_B = 1$). We assume that R_2 is the hot bath, while R_1 is the cold bath, with $\beta_{R_2} =: \beta_2 \leqslant \beta_{R_1} =: \beta_1$.

The interaction Hamiltonian between the working qubits and their respective thermal reservoirs, denoted by $\hat{H}_{S_{12}R}$, is given by

$$\hat{H}_{S_{12}R} = \sum_{m=1}^{2} \sum_k g_{mk} (\hat{\sigma}^+_m \otimes \hat{a}_{mk} + \hat{\sigma}^-_m \otimes \hat{a}^\dagger_{mk}). \tag{7}$$

In our analysis, we assume weak coupling between the baths and the working qubits and employ the standard local Born-Markov master equation in Lindblad form [39–41]

$$\frac{d}{dt} \hat{\rho}_T(t) = -i[\hat{H}_T, \hat{\rho}_T(t)] + \mathcal{L}[\hat{\rho}_T(t)], \tag{8}$$

where the first term is for the Liouville-von Neumann evolution and $\mathcal{L}[\hat{\rho}_T(t)]$ accounts for the Lindbladian evolution.

The quantum master equation in Eq. (8) describes the dynamics for any type of Markovian reservoir, whether bosonic or fermionic. The dissipator $\mathcal{D}[\hat{\rho}_T(t)]$ for the bosonic reservoirs is expressed as

$$\mathcal{L}[\hat{\rho}_T(t)] = \sum_{m=1}^{2} \mu_m (\bar{n}_m \mathcal{D}[\sigma^+_m] \hat{\rho}_T(t) + (\bar{n}_m + 1) \mathcal{D}[\sigma^-_m] \hat{\rho}_T(t)), \tag{9}$$

where μ_m is the dissipation rate, and the Lindblad dissipator superoperator, acting on a density matrix $\hat{\rho}$, for a jump operator $\hat{o}$ is defined as $\mathcal{D}[\hat{o}]\hat{\rho} := \hat{o}\hat{\rho}\hat{o}^\dagger - \{\hat{o}^\dagger \hat{o}, \hat{\rho}\}/2$, with the second term representing the anticommutator. The mean number of quanta $\bar{n}_m$ in each reservoir R_m with $m = \{1, 2\}$, on resonance with the corresponding qubit, is given by

$$\bar{n}^\pm_m = \frac{1}{e^{\beta_m E_{S_m}} \pm 1}, \tag{10}$$

with the superscript $+$ and $-$ distinguishing the fermionic and bosonic character of the reservoirs.

The total initial state of the entire system including the reservoirs is assumed to be factorized as

$$\hat{\rho}(0) = \hat{\rho}_{R_1 S_1}(0) \otimes \hat{\rho}_{R_2 S_2}(0) \otimes \rho_0(0), \tag{11}$$

where $\hat{\rho}_0(0)$ represents the initial density matrix of the work qubit S_0. Moreover, $\hat{\rho}_{R_1 S_1}(0) = \hat{\rho}_{R_1}(0) \otimes \hat{\rho}_1(0)$ and $\hat{\rho}_{R_2 S_2}(0) = \hat{\rho}_{R_2}(0) \otimes \hat{\rho}_2(0)$, where $\hat{\rho}_1(0)$ and $\hat{\rho}_2(0)$ are the initial density matrices of the qubits S_1 and S_2, respectively.

Based on the structure of the Hamiltonian and the master equation, we can anticipate how the work qubit S_0 will evolve concerning the initial conditions. Moreover, the thermal noise from the Markovian reservoirs is filtered by the QATM qubits $S_{12} = S_1 \otimes S_2$ during the heat transfer process. Effectively, transforming the combined QATM qubits $S_{12} = S_1 \otimes S_2$ and their attached reservoirs into structured baths for the work qubit S_0. These baths exhibit effective Lorentzian linewidths, resulting in non-Markovian dynamics for the work qubit S_0.

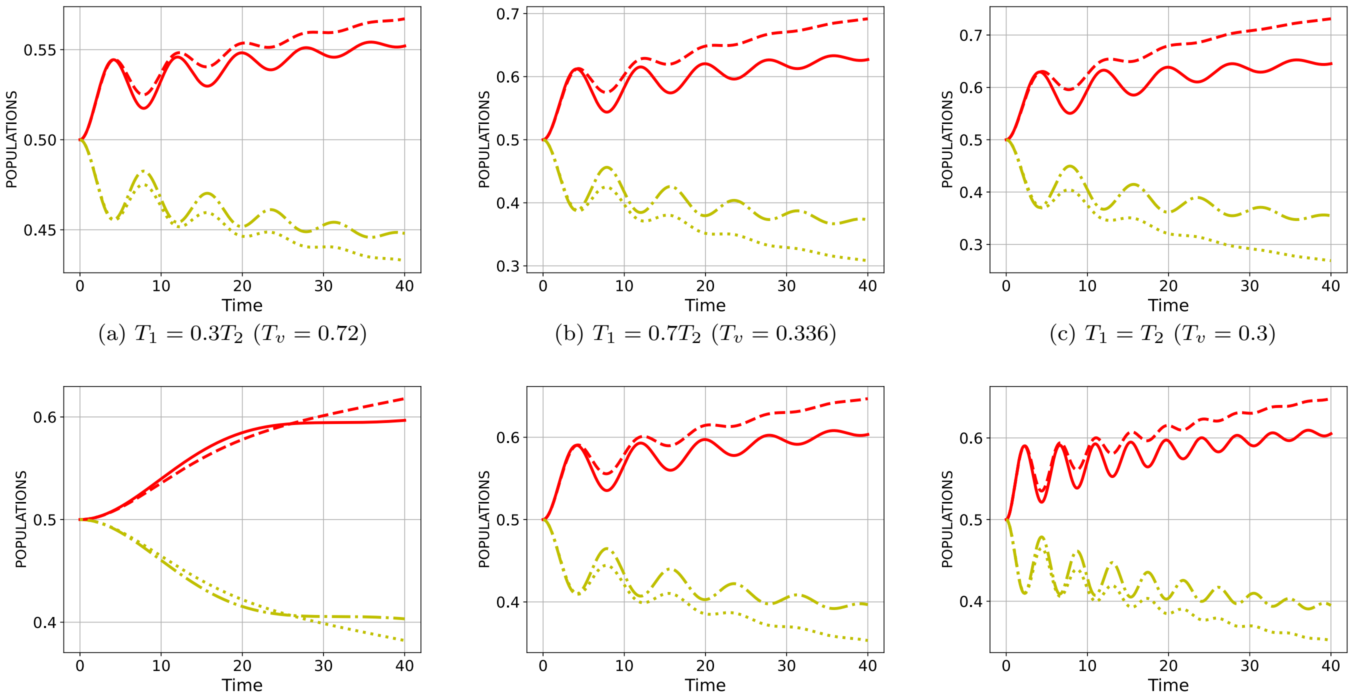

(a) $T_1 = 0.3T_2$ ($T_v = 0.72$) (b) $T_1 = 0.7T_2$ ($T_v = 0.336$) (c) $T_1 = T_2$ ($T_v = 0.3$)

(d) $k = 0.1$ (e) $k = 0.5$ (f) $k = 0.9$

FIG. 2. Plots of the populations of the work qubit S_0. The red (solid line, dashed line) curves represent the ground state for the (fermionic, bosonic) reservoirs, while the yellow (dash-dot line, dotted line) curves correspond to the excited state for the (fermionic, bosonic) reservoirs. In (a)–(c), we set $k = 0.5$ for different values of the temperature T_1 of the qubit S_1. In (d)–(f), we set $T_1 = 0.5T_2$ for various couplings k between S_{12} and S_0.

Under such non-Markovian evolution, the interaction-induced coherence will be temporarily stored in S_0. In the following analysis, we will evolve the initial state and trace out the QATM qubits S_{12} to investigate the dynamics of the work qubit S_0. This will allow us to verify our interpretation of the interaction between S_{12} and S_0, and to identify the signature of non-Markovianity, information generation, and storage in the work qubit S_0. In addition, we will examine the Landauer bound and generalized Landauer bound of the proposed system.

III. RESULTS

In this section, we present the results of our analysis, starting with the initial assumptions. We assume that the qubits are initially uncorrelated and that the working qubits are in thermal equilibrium with their respective heat baths, described by the state

$$\hat{\rho}_{S_{12}}(0) = \hat{\rho}_1 \otimes \hat{\rho}_2 = \frac{1}{Z_1} e^{-\beta_1 \hat{H}_1} \otimes \frac{1}{Z_2} e^{-\beta_2 \hat{H}_2}, \tag{12}$$

where $Z_m = \mathrm{Tr}[\exp(-\beta_m \hat{H}_m)]$ is the partition function. We take the initial state of S_0 to be S_0 is $|\psi\rangle_0(0) = \frac{1}{2}(|0_{S_0}\rangle + |1_{S_0}\rangle)$. For our analysis, we normalize the energy scale using $E_{S_2} = 1$ and set the parameters as $E_{S_1} = 0.2$, $\mu_1 = 0.1$, $\mu_2 = 0.1$, and $T_2 = 0.3$.

A. QATM operation on work qubit

We evolve the initial state by solving the master equation using Eqs. (8) and (9), and we compute the dynamics of the populations and coherence in the reduced state of the work qubit S_0. The coherence is quantified using the relative entropy of coherence (REC), also known as the Kullback-Leibler divergence [43,44]. Indeed, the REC in our scenario, namely, $C(\hat{\rho}(t))$ turns out to be [42]

$$C(\hat{\rho}_0(t)) = S(\hat{\rho}_0(t) \| \tilde{\rho}_0(t)), \tag{13}$$

where $S(\hat{\rho}_0(t) \| \tilde{\rho}_0(t))$ is the relative entropy. Here, $\tilde{\rho}_0$ is the fully dephased state, representing the density matrix of the work qubit S_0 without its off-diagonal elements.

In Figs. 2(a)–2(c), we plot the populations of S_0 while varying the temperatures and quantum statistics of the reservoirs T_1 and T_2. The results show clear oscillatory behavior in the populations, indicating the influence of the QATM (S_{12}) on the population dynamics of S_0. Figures 2(d)–2(f) illustrate the effect of varying the coupling constant k on the population dynamics of S_0. Here, we observe that reducing the coupling between S_0 and the QATM (S_{12}) dampens the oscillations, confirming that the interaction between S_0 and S_{12} is responsible for these oscillations.

Figure 3 shows the coherence of S_0 as a function of time, measured by the relative entropy of coherence. In Fig. 3(a), we manipulate the coherence dynamics by varying the temperature of the reservoirs T_1 and T_2. The results indicate that the coherence of S_0 decays over time due to the decoherence

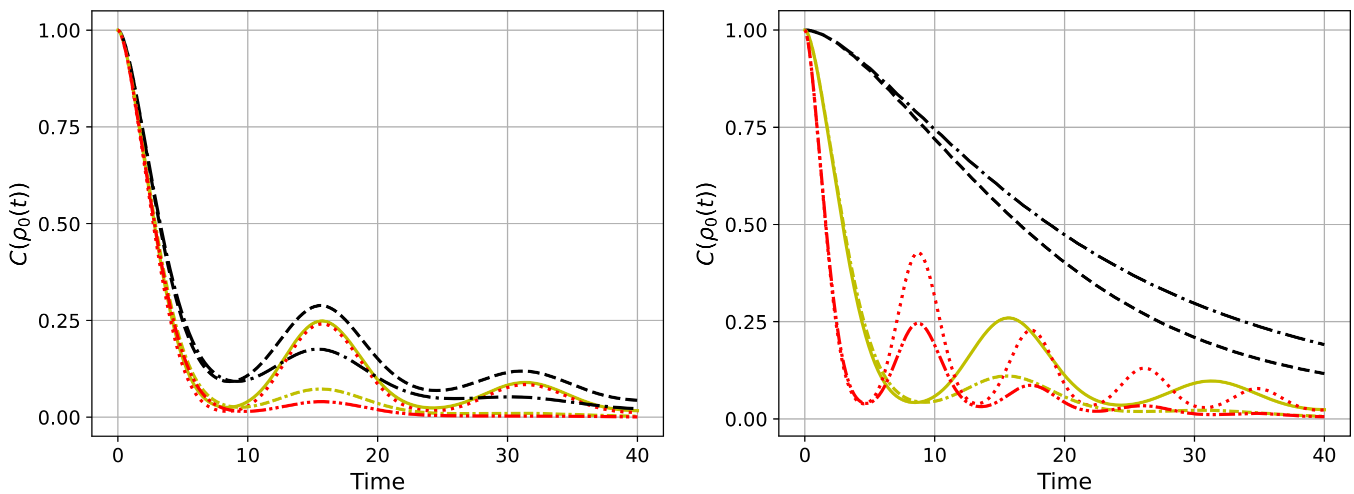

FIG. 3. Plots of the relative entropy of coherence $C(\rho_0(t))$ for the work qubit S_0 as a function of time. In (a), we vary the resonance temperature between T_1 and T_2, where the black (dashed line, dash-dot line), yellow (solid line, dash-dash-dot line), and red (dotted line, dot-dot-dash line) curves representing $T_1 = 0.3T_2$, $0.7T_2$, and T_2, respectively, for (fermionic, bosonic) reservoirs. Besides, we set $k = 0.5$. In (b), we vary the coupling k between S_0 and S_{12}, with the black (dashed line, dash-dot line), yellow (solid line, dash-dash-dot line), and red (dotted line, dot-dot-dash line) curves corresponding to $k = 0.1$, 0.5, and 0.9, respectively, for (fermionic, bosonic) reservoirs. In this case, we set $T_1 = 0.5T_2$.

induced by reservoirs R_1 and R_2. The nonmonotonic decrease in the relative entropy of coherence suggests a backflow of information between S_{12} and S_0, a characteristic of non-Markovian behavior. Additionally, in Fig. 3(b), we find that a strong coupling strength k induces a transition from a Markovian to a non-Markovian regime. Specifically, the subsystems S_1 and S_2, together with their respective reservoirs R_1 and R_2, act as structured reservoirs relative to the qubit S_0.

The observed coherence and population oscillations of S_0 can be interpreted as follows: the QATM system S_{12} functions as an information engine that rectifies thermal fluctuations and chaotic energy (heat) into coherent oscillations of S_0. These coherent oscillations of S_0 can subsequently be converted into other forms of energy, such as radiation from dipole oscillation. Thus an information engine like this could potentially be harnessed as a compact quantum technological device for generating useful energy.

B. Non-Markovian character of QATM action on work qubit dynamics

To further explore the information dynamics in the reduced density matrix $\hat{\rho}_0$, we evaluate the trace distance of S_0 to analyze potential memory effects. This section focuses on examining the non-Markovian nature of the proposed model by quantifying the amount of exchanged information between the open system S_0 and the thermal machine S_{12}. The analysis is carried out using trace distance and mutual information as key indicators.

1. Trace distance

In the theory of open quantum systems, the trace distance is a well-established metric for detecting non-Markovian dynamics [45,48]. Consider two quantum states of the system S_0, denoted by $\hat{\rho}_0^A$ and $\hat{\rho}_0^B$. The trace distance between these states, denoted by $D(\hat{\rho}_0^A(t), \hat{\rho}_0^B(t))$, is defined a

$$D(\hat{\rho}_0^A(t), \hat{\rho}_0^B(t)) = \tfrac{1}{2}||\hat{\rho}_0^A(t) - \hat{\rho}_0^B(t)||. \tag{14}$$

where $\|\cdot\|$ represents the trace norm. Physically, this quantity measures how distinguishable the two states $\hat{\rho}_0^A(t)$ and $\hat{\rho}_0^B(t)$ are over time. If $D(\hat{\rho}_0^A(t), \hat{\rho}_0^B(t))$ decreases monotonically over time, the evolution of S_0 is classified as Markovian. Conversely, if this measure exhibits non-monotonic behavior, the dynamics are indicative of non-Markovianity.

We explore the non-Markovianity of QATM by examining the trace distance in two scenarios: one involving bosonic reservoirs and the other involving fermionic reservoirs. In the first scenario, we calculate the trace distance between two superposition states, $|\psi_A\rangle_0 = (|0_{S_0}\rangle + |1_{S_0}\rangle)/\sqrt{2}$ and $|\psi_B\rangle_0 = (|0_{S_0}\rangle - |1_{S_0}\rangle)/\sqrt{2}$, where $\hat{\rho}_0^{A/B} = |\psi_{A/B}\rangle_0 \langle\psi_{A/B}|$. Furthermore, we quantify non-Markovianity in the second scenario using a pair of states, $\hat{\rho}_0^A = |1_{S_0}\rangle\langle 1_{S_0}|$ and $\hat{\rho}_0^B = |0_{S_0}\rangle\langle 0_{S_0}|$. In both cases, we examine the effect of the coupling constant k in the Hamiltonian $\hat{H}_{S_{12}S_0}$ and the bath temperatures on the trace distance and the emergence of non-Markovian effects.

In Fig. 4(a), we plot the trace distance between $|\psi_A\rangle_0$ and $|\psi_B\rangle_0$ over time, focusing on the effect of varying the resonance reservoir temperatures $T1$ and T_2. The trace distance is analyzed for QATM qubits S_{12} coupled to either fermionic (dashed line, solid line, dotted line) or bosonic (dash-dot line, dash-dash-dot line, dot-dot-dash line) reservoirs R_1 and R_2. The nonmonotonic behavior of the trace distance indicates that the evolution of the S_0 is non-Markovian. Notably, the bath temperatures influence the degree of non-Markovianity.

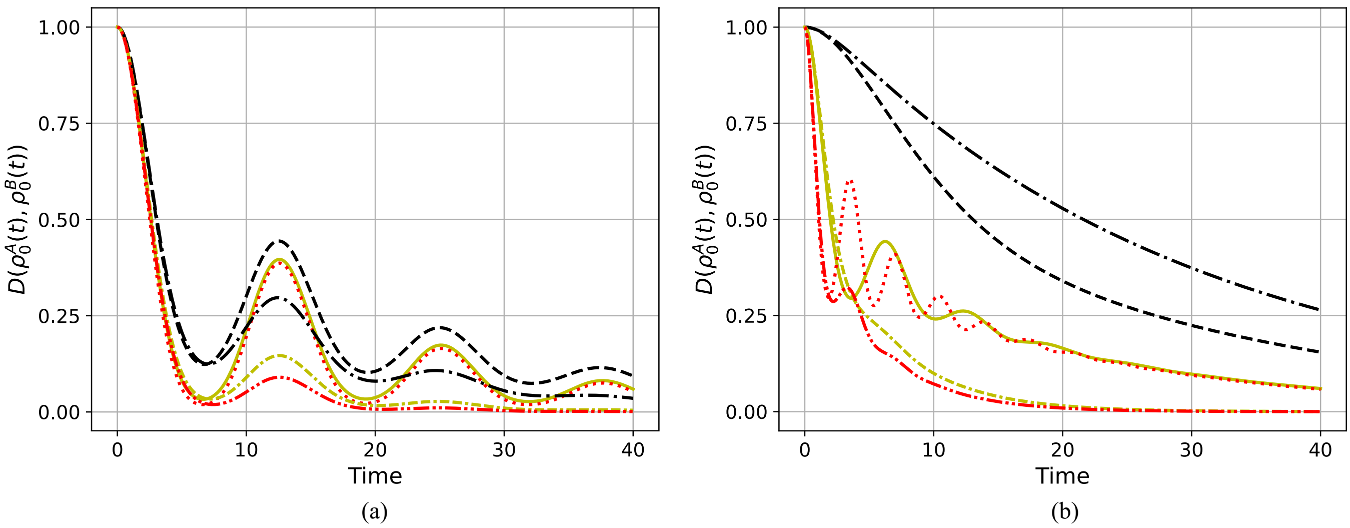

FIG. 4. Plots of the trace distance $D(\hat{\rho}_0^A(t), \hat{\rho}_0^B(t))$ of the work qubit S_0 versus time. (a) Trace distance between $|\psi_A\rangle_0$ and $|\psi_B\rangle_0$, where we manipulate the resonance temperature between T_1 and T_2, where black (dashed line, dash-dot line), yellow(solid line, dash-dash-dot line) and red (dotted line, dot-dot-dash line) reflect $T_1 = 0.3T_2$, $T_1 = 0.7T_2$, and $T_1 = T_2$ respectively for (fermionic, bosonic) reservoirs, and we set $k = 0.5$. (b) Trace distance between $|1\rangle_0$ and $|0\rangle_0$, where we manipulate the coupling k between S_0 and S_{12}, where black (dashed line, dash-dot line), yellow (solid line, dash-dash-dot line), and red (dotted line, dot-dot-dash line) reflect $k = 0.1$, 0.5, and 0.9 respectively for (fermionic, bosonic) reservoirs, and we set $T_1 = 0.5T_2$.

Specifically, an increase in backflow is observed when $T_1 < T_2$, while raising T_1 tends to reduce the degree of backflow between the reservoirs and the open system S_0.

In Fig. 4(b), we examine the trace distance for the subsystem S_0 between the initial states $|1_{S_0}\rangle\langle 1_{S_0}|$ and $|0_{S_0}\rangle\langle 0_{S_0}|$ over time, varying the coupling between S_0 and the thermal machine S_{12}. This analysis considers both fermionic and bosonic reservoirs. A clear transition from Markovian to non-Markovian dynamics is observed as the coupling constant k increases. Indeed, stronger coupling between S_0 and S_{12} drives the system dynamics from the Markovian to the non-Markovian regime.

Now, we manipulate the trace distance between the states of the QATM S_{12} over time. We consider two states of the subsystem S_{12}, namely, $\hat{\rho}_{12}^A$ when the density matrix of work qubit is $\hat{\rho}_0^A$; and $\hat{\rho}_{12}^B$ when the state of the work qubit is $\hat{\rho}_0^B$. Then, the trace distance of the QATM is defined as

$$D\big(\hat{\rho}_{12}^A(t), \hat{\rho}_{12}^B(t)\big) = \tfrac{1}{2}\big\|\hat{\rho}_{12}^A(t) - \hat{\rho}_{12}^B(t)\big\|. \qquad (15)$$

In Fig. 5, we plot the trace distance of the QATM S_{12} over time. In Fig. 5(a), we depict the trace distance between $\hat{\rho}_{12}^A(t)$ and $\hat{\rho}_{12}^B(t)$, where the work qubit S_0 is initially prepared in the states $|\psi_A\rangle_0$ and $|\psi_B\rangle_0$, respectively. Similarly, in Fig. 5(b), we show the trace distance between $\hat{\rho}_{12}^A(t)$ and $\hat{\rho}_{12}^B(t)$, where the work qubit S_0 is initially in the states $|1\rangle_0$ and $|0\rangle_0$, respectively. Initially, we observe that the trace distance is vanished, namely, $D(\hat{\rho}_{12}^A(0), \hat{\rho}_{12}^B(0)) = 0$ since $\hat{\rho}_{12}^A(0) = \hat{\rho}_{12}^B(0)$. For $t > 0$, the trace distance of the QATM S_{12} increases nonmonotonically. This behavior indicates that the trace distance of the work qubit decreases nonmonotonically, which implies that information is transferred from the work qubit S_0 to the QATM S_{12}. Additionally, we observe that when the trace distance of the QATM S_{12} decreases, the trace distance of the work qubit S_0 increases. This suggests that there exists a backflow of information between the QATM S_{12} and the work qubit S_0 over time. Indeed, the transfer of information between them is partial due to the decoherence effects of reservoirs R_1 and R_2.

Figures 4(a), 4(b), 5(a), and 5(b) demonstrate how the interaction between the thermal machine and the reservoirs (both bosonic and fermionic) impacts the dynamics of the open system S_0. The bosonic reservoir exhibits greater temperature sensitivity compared to the fermionic reservoirs, leading to a more rapid reduction of non-Markovianity [49]. In the nonequilibrium regime, QATM effectively manages non-Markovian dynamics by acting as an intermediary system between the reservoirs R_1-R_2 and the work qubit S_0. demonstrate how the interaction between the thermal machine and the reservoirs (both bosonic and fermionic) impacts the dynamics of the open system S_0. The bosonic reservoir exhibits greater temperature sensitivity compared to the fermionic reservoirs, leading to a more rapid reduction of non-Markovianity [49]. In the nonequilibrium regime, QATM effectively manages non-Markovian dynamics by acting as an intermediary system between the reservoirs R_1-R_2 and the work qubit S_0.

2. Mutual information

We also examine the mutual information between the thermal machine and the open system to provide further insights into these memory effects. We employ the concept of mutual information [46] to quantify the information shared between the work qubit S_0 and the QATM working qubits S_{12}. Mutual information measures the amount of shared information between two systems using the von Neumann entropy of each

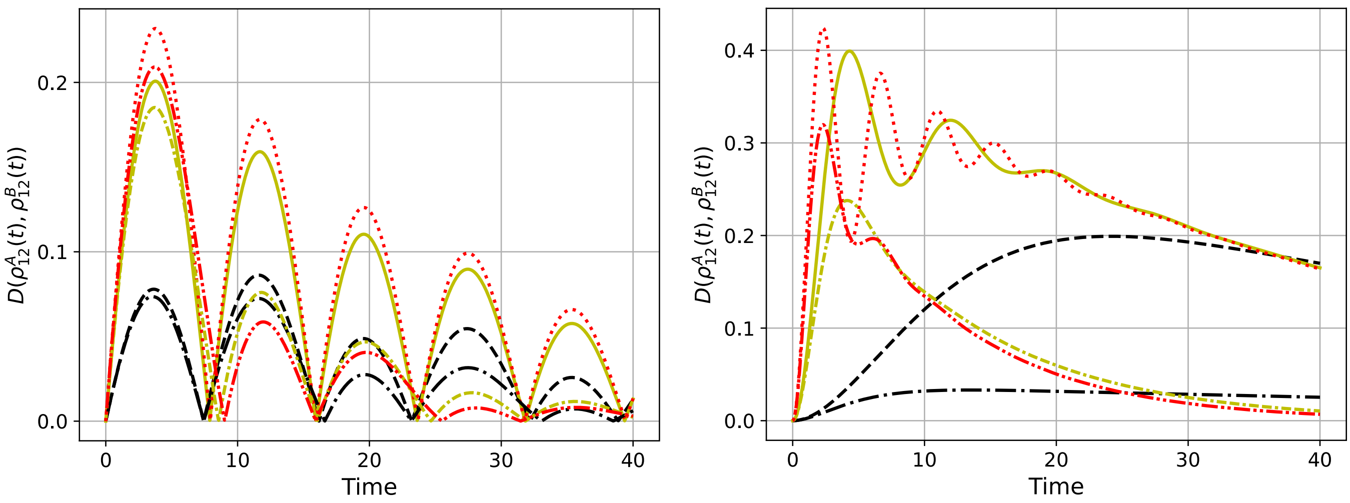

FIG. 5. Plots of the trace distance $D(\rho_{12}^A(t), \rho_{12}^B(t))$ of the QATM S_{12} versus time. (a) Trace distance between $\rho_{12}^A(t)$ where S_0 is prepared initially in $|\psi_A\rangle_0$ and $\rho_{12}^B(t)$ where S_0 is prepared initially in $|\psi_B\rangle_0$. Moreover, we manipulate the resonance temperature between T_1 and T_2, where black (dashed line, dash-dot line), yellow(solid line, dash-dash-dot line) and red (dotted line, dot-dot-dash line) reflect $T_1 = 0.3T_2$, $0.7T_2$, and T_2 respectively for (fermionic, bosonic) reservoirs, and we set $k = 0.5$. (b) Trace distance between $\rho_{12}^A(t)$ where S_0 is prepared initially in $|1\rangle_0$ and $\rho_{12}^B(t)$ where S_0 is prepared initially in $|0\rangle_0$. Moreover, we manipulate the coupling k between S_0 and S_{12}, where black (dashed line, dash-dot line), yellow(solid line, dash-dash-dot line) and red (dotted line, dot-dot-dash line) reflect $k = 0.1$, 0.5, and 0.9 respectively for (fermionic, bosonic) reservoirs. Besides, we set $T_1 = 0.5T_2$.

subsystem. For our subsystems S_0 and S_{12}, the von Neumann entropy is defined as

$$S(\hat{\rho}_0(t)) = -\mathrm{Tr}\{\hat{\rho}_0(t)\log_2(\hat{\rho}_0(t))\}, \tag{16}$$

$$S(\hat{\rho}_{12}(t)) = -\mathrm{Tr}\{\hat{\rho}_{12}(t)\log_2(\hat{\rho}_{12}(t))\}. \tag{17}$$

The von Neumann entropy of the total system $T = \{S_1 \otimes S_2 \otimes S_0\}$ is given by $S(\hat{\rho}_T(t)) = -\mathrm{Tr}\{\hat{\rho}_T(t)\log_2(\hat{\rho}_T(t))\}$. Thus, the mutual information between S_0 and S_{12} is

$$I(t) = S(\hat{\rho}_0(t)) + S(\hat{\rho}_{12}(t)) - S(\hat{\rho}_T(t)). \tag{18}$$

We investigate the mutual information when the thermal machine interacts with bosonic and fermionic reservoirs. We consider two cases: the work qubit S_0 initially prepared in a superposition state $|\psi_A\rangle_0 = \frac{1}{\sqrt{2}}(|0_{S_0}\rangle + |1_{S_0}\rangle)$, and in a state $|1_{S_0}\rangle$. The mutual information is analyzed over time by varying the reservoir temperatures T_1 and T_2. Additionally, for the initial state $|1_{S_0}\rangle$, we study the impact of altering the coupling between S_0 and S_{12}.

In Fig. 6, the behavior of the mutual information between the subsystem S_0 and the thermal machine S_{12} is shown over time. The thermal machine is coupled to fermionic and bosonic reservoirs. In Fig. 6(a), we plot the mutual information where the system S_0 is initially prepared in the superposition state $|\psi_A\rangle_0$ under various temperatures of the reservoirs T_1 and T_2. The thermal machine remains coupled to fermionic and bosonic reservoirs. Initially, the mutual information is zero, but it increases nonmonotonically over time, indicating an increase in the information shared between S_0 and the thermal machine, signaling backflow between them. The effect of the temperature T_1 and T_2 is evident; the increase in mutual information is attributed to the rising temperature T_1 resonating with T_2 in both bosonic and fermionic cases.

In Fig. 6(b), the mutual information is plotted for the initial state $|1_{S_0}\rangle$ under various settings of the coupling constant k between S_0 and S_{12}. Initially, there is no correlation, but as the dynamics evolve ($t > 0$), the mutual information increases nonmonotonically over time for strong coupling k. However, when the coupling k is reduced, the mutual information evolves monotonically, reflecting the Markovian dynamics of the system.

Figures 4 and 6 show that the mutual information between the thermal machine and the bosonic reservoir (dashed line, solid line, dotted line) is generally less than that obtained with the fermionic reservoir (dash-dot line, dash-dash-dot line, dot-dot-dash line), due to the temperature sensitivity of bosonic reservoirs. The possibility of controlling coherence and decoherence is linked to the specific choice of system parameters, particularly bath temperatures, qubit energy spacings, and coupling strength k.

C. Information backflow between work qubit and QATM and the Landauer bound

Finally, we demonstrate that non-Markovianity can violate the conventional Landauer bound, but a generalized lower bound can be established. Landauer's principle is a fundamental concept rooted in thermodynamics and quantum information, positing that information loss over time, due to interactions between an open system and its environment, necessitates a minimum energy expenditure to reset this information [50].

Assume that the qubits of QATM, namely, S_1 and S_2 are in thermal contact with reservoirs R_1 and R_2. In this inspiration, the composite system S_{12} forms then a single system. Indeed, this system is coupled to a virtual reservoir, denoted as R_{12}, operating at the virtual temperature T_v, as shown

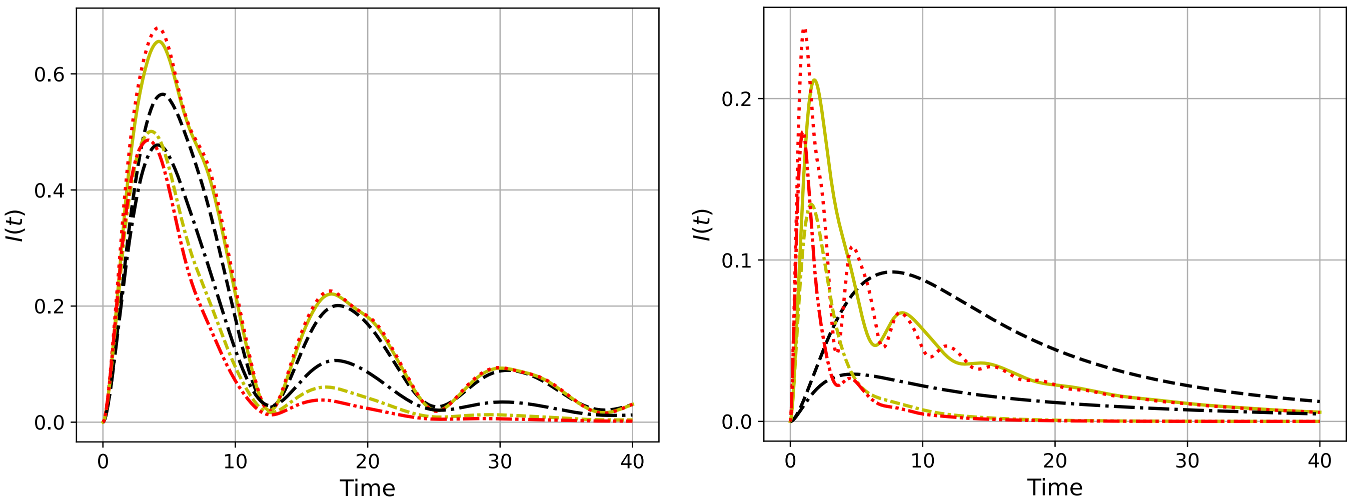

(a) (b)

FIG. 6. Plots of the mutual information $I(t)$ between the work qubit S_0 and the QATM S_{12} vs time. In (a), S_0 and S_{12} are initially prepared in $|\psi_A\rangle_0$ and $\hat{\rho}S_{12}$, respectively, for various considerations of the resonance temperature between T_1 and T_2. The black (dashed line, dash-dot line), yellow (solid line, dash-dash-dot line), and red (dotted line, dot-dot-dash line) curves correspond to $T_1 = 0.3T_2$, $0.7T_2$, and T_2, respectively, for (fermionic, bosonic) reservoirs. Moreover, we set $k = 0.5$. In (b), we consider the initial states of S_0 and S_{12} as $\hat{1}0$ and $\hat{\rho}S_{12}$, respectively, for various coupling k between S_0 and S_{12}. The black (dashed line, dash-dot line), yellow (solid line, dash-dash-dot line), and red (dotted line, dot-dot-dash line) curves correspond to $k = 0.1$, 0.5, and 0.9, respectively, for (fermionic, bosonic) reservoirs. Besides, we set $T_1 = 0.5T_2$.

in Fig. 7. The transitions corresponding to the blue energy spacing E_1 are associated with the interaction between S_1 and reservoir R_1. In contrast, the transitions corresponding to the red energy spacing E_2 are linked to the interaction between S_2 and reservoir R_2. According to the interaction Hamiltonian between the QATM S_{12} and the work qubit S_0 given in Eq. (4), transitions are imposed from $|0_{S_1}1_{S_2}0_{S_0}\rangle\langle 1_{S_1}0_{S_2}1_{S_0}|$ and their Hermitian conjugate $|1_{S_1}0_{S_2}1_{S_0}\rangle\langle 0_{S_1}1_{S_2}0_{S_0}|$. These interactions occur only within the resonance region where the work qubit S_0, with spacing energy $E_{S_0} = E_{S_2} - E_{S_1}$, interacts with the QATM, which acts as a single entity with spacing energy $E_{S_{12}} = E_{S_0}$.

Assume that $|0_{S_{12}}\rangle = |1_{S_1}0_{S_2}\rangle$ is the first ground state of the QATM's qubits, with the population $P_0^{S_{12}} = P_1^{S_1}P_0^{S_2}$, as illustrated in Fig. 7. The second excited state is denoted as $|1_{S_{12}}\rangle = |0_{S_1}1_{S_2}\rangle$ with a population $P_1^{S_{12}} = P_0^{S_1}P_1^{S_2}$. The spacing energy between these states is $E_{S_{12}} = E_{S_2} - E_{S_1}$, which is in resonance with the work qubit S_0. Moreover, S_1 and S_2 in the context of the Boltzmann distribution, satisfies the relation:

$$P_1^{S_m} = P_0^{S_m} \mathrm{e}^{-E_m/T_m} \quad (m = 1, 2). \tag{19}$$

The ratio between the corresponding populations of the QATM S_{12} is then leads to the definition of T_v using

$$\frac{P_1^{S_{12}}}{P_0^{S_{12}}} = \frac{P_0^{S_1}P_1^{S_2}}{P_1^{S_1}P_0^{S_2}} =: \mathrm{e}^{-E_{S_{12}}/T_v}. \tag{20}$$

Therefore, by using Eqs. (19) and (20), the virtual temperature of the thermal machine can be introduced as

$$T_v = \frac{E_{S_{12}}}{E_{S_2}/T_2 - E_{S_1}/T_1}. \tag{21}$$

Accordingly, the virtual temperature does not represent a simple average between T_1 and T_2. Notably, in the case of equilibrium where $T_1 = T_2$, the virtual temperature simplifies to $T_v = T_1 = T_2$. Physically, the interaction Hamiltonian $\hat{H}_{S_{12}S_0}$ indicates that the QATM (S_{12}) operates as a single body interacting with the work qubit S_0 according to the following Hamiltonian:

$$\hat{H}_{S_{12}S_0} = k\big(|0_{S_{12}}1_{S_0}\rangle\langle 1_{S_{12}}0_{S_0}| + \text{H.c.}\big). \tag{22}$$

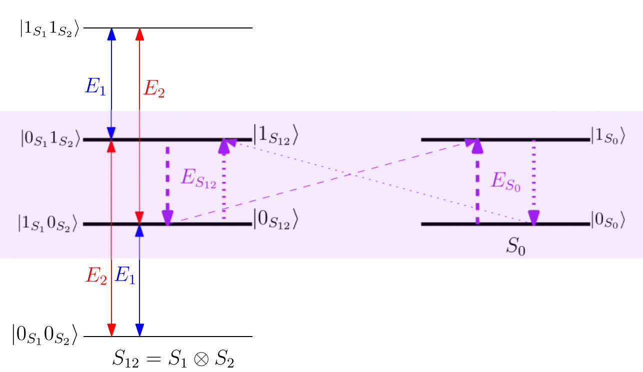

FIG. 7. A schematic representation of the QATM $S_{12} = S_1 \otimes S_2$, modeled as a single body S_{12} with ground and excited states $|0_{S_{12}}\rangle$ and $|1_{S_{12}}\rangle$, respectively. The energy spacing is $E_{S_{12}} = E_{S_2} - E_{S_1}$, where the virtual temperature is T_v. Moreover, the QATM is coupled to the work qubit S_0. The purple region highlights the thermal contact between the work qubit, QATM, and the reservoirs R_1 and R_2 at the virtual temperature T_v.

As mentioned, our theoretical model considers that the work qubit S_0 is coupled to the QATM S_{12}. Furthermore, S_{12} is in thermal contact with the virtual reservoir R_{12} at the virtual temperature T_v. Consequently, the total system $T = S_{12} \otimes S_0$ is in thermal contact with the virtual reservoir R_{12} at T_v. Here, the energy current of the total system T, namely, $\dot{E}_T(t) = \frac{d}{dt}\mathrm{tr}\{\hat{H}_T\hat{\rho}_T(t)\}$ which consists of two parts: the variation of

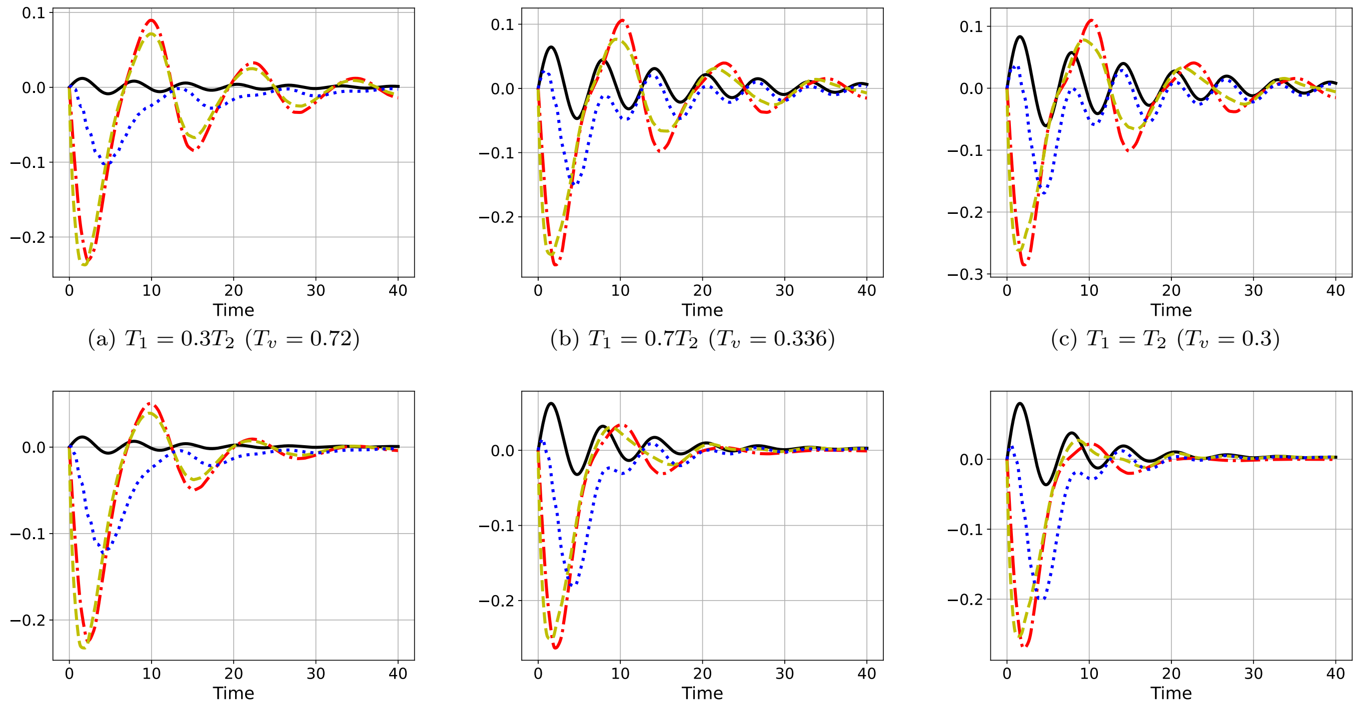

(a) $T_1 = 0.3T_2$ $(T_v = 0.72)$ (b) $T_1 = 0.7T_2$ $(T_v = 0.336)$ (c) $T_1 = T_2$ $(T_v = 0.3)$

(d) $T_1 = 0.3T_2$ $(T_v = 0.72)$ (e) $T_1 = 0.7T_2$ $(T_v = 0.336)$ (f) $T_1 = T_2$ $(T_v = 0.3)$

FIG. 8. Plots of the heat flux $\beta_v \dot{Q}_{S_0}$ (black solid line), exchanged entropy $\Delta\dot{S}_0 = \Delta\dot{S}(\hat{\rho}_0(t))$ (yellow dashed line), generalized Landauer bound (GLB) (blue dotted line), and the derivative of the trace distance $\sigma(t)$ (red dash-dot line), when the work qubit S_0 is initially prepared in the state $|\psi_A\rangle_0$. (a)–(c) and (d)–(f) correspond to the cases of fermionic and bosonic reservoirs, respectively. We set $k = 0.5$.

heat current, namely $\dot{Q}_T(t)$ and the variation of extractable work, i.e., $\dot{W}_T(t)$, as described in Refs. [32,59,60],

$$\dot{E}_T(t) = \dot{Q}_T(t) + \dot{W}_T(t), \tag{23}$$

$$\dot{Q}_T(t) = \mathrm{tr}\left\{\hat{H}_T \frac{d}{dt}\hat{\rho}_T(t)\right\}, \tag{24}$$

$$\dot{W}_T(t) = \mathrm{tr}\left\{\hat{\rho}_T(t)\frac{d}{dt}\hat{H}_T\right\}. \tag{25}$$

In our scenario, the Hamiltonian $\hat{H}_T$ in Eq. (2) is time-independent, that is, $\frac{d}{dt}\hat{H}_T = 0$ which implies that the extracted work of our theoretical model has vanished, namely $W_T(t) = 0$. Consequently, the change in internal energy is solely due to heat exchange with the reservoir R_{12}. This means that the energy current in our model coincides with the heat current since no external work is performed. Therefore

$$\dot{E}_T(t) = \dot{Q}_T(t). \tag{26}$$

Physically speaking, in our case no coherent-driving forces are used to operate the QATM S_{12}. this confirms that our thermal machine is truly autonomous and does not require any external energy input to be operated.

In this regard, Landauer's principle constrains heat dissipation in reservoirs R_1 and R_2 by reducing the information employing entropy of the overall system T. Notably, the conventional Landauer limit applies universally to the entire system T [35,50,51]. Our analysis shows that the interaction Hamiltonian in Eq. (22) indicates that the total system, $T = S_{12} \otimes S_0$, is in thermal contact with the virtual reservoir R_{12} at the virtual temperature T_v. Consequently, the heat flux exchanged between the total system T and the virtual reservoir R_{12}, denoted as $\dot{Q}_T(t)$, is governed by the virtual temperature T_v over time. This leads to the following Landauer bound:

$$\beta_v \dot{Q}_T(t) \geqslant \Delta\dot{S}(\hat{\rho}_T(t)), \tag{27}$$

where $\beta_v = 1/T_v$. The rate of entropy change between the total system T and the reservoirs R_1 and R_2 is given by [52]

$$\Delta\dot{S}(\hat{\rho}_T(t)) = \frac{d}{dt}[S(\hat{\rho}_T(0)) - S(\hat{\rho}_T(t))] = -\dot{S}(\hat{\rho}_T(t)), \tag{28}$$

where $S(\hat{\rho}_T) = -\mathrm{Tr}\{\hat{\rho}_T \log \hat{\rho}_T\}$ is the von Neumann entropy of the density matrix $\hat{\rho}_T$.

In the Markovian regime, the Landauer bound in Eq. (27) holds at all times during the interaction between S_0, S_{12}, and the reservoirs R_1 and R_2. However, the non-Markovian dynamics can lead to a violation of the Landauer bound [53,54], as this bound is defined solely in the context of information erasure during an irreversible transformation. The backflow of information between the system S_0 and the reservoirs R_1 and R_2, mediated by the system S_{12}, indicates the presence of memory effects (i.e., a semireversible transformation). Since the effective thermal contact at T_v behaves like a finite size reservoir for the work qubit (or adding a working qubit before a Markovian bath to realize a structured bath) it attributes a finite size character to the effective reservoir for the working qubit. Landauer limit can change due to finite-size corrections [55]. Accordingly, a generalized bound is required in our analysis as well.

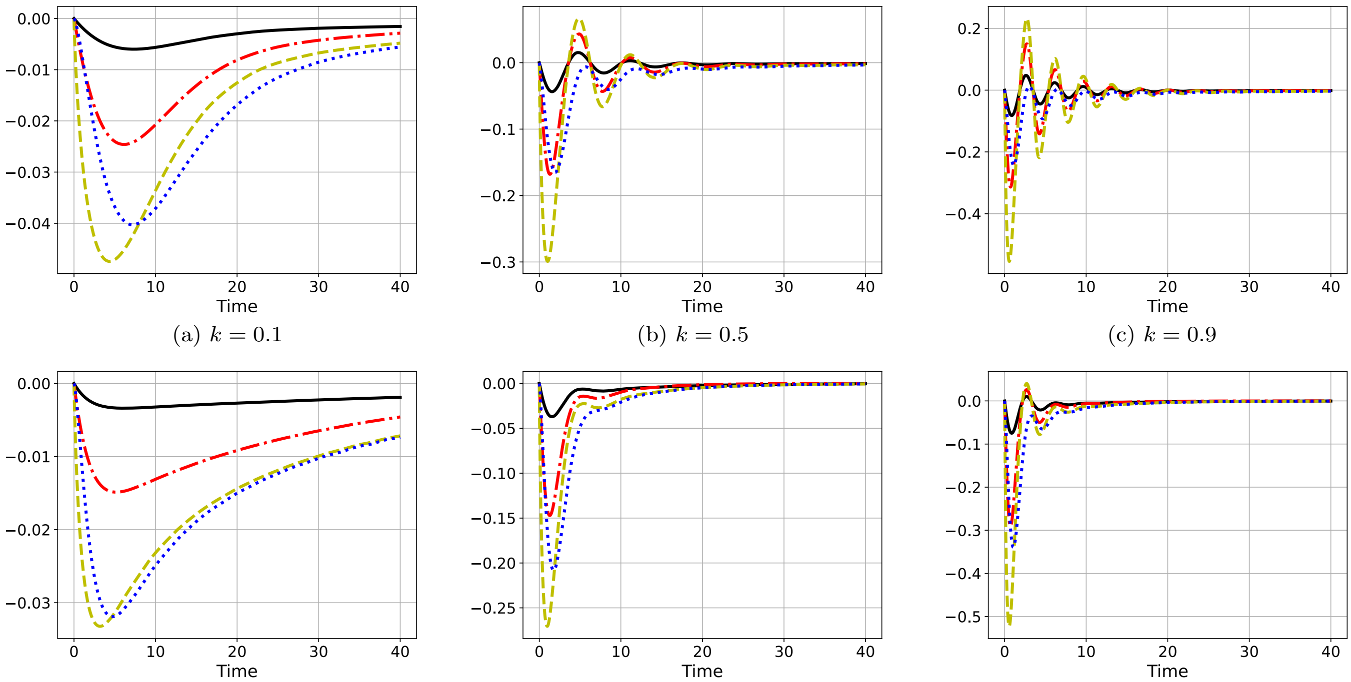

(a) $k = 0.1$ (b) $k = 0.5$ (c) $k = 0.9$

(d) $k = 0.1$ (e) $k = 0.5$ (f) $k = 0.9$

FIG. 9. Plots of heat flux $\beta_v \dot{Q}_{S_0}$ (black solid line), exchanged entropy $\Delta\dot{S}_0 = \Delta\dot{S}(\hat{\rho}_0(t))$ (yellow dashed line), generalized lower Landauer bound (GLB) (blue dotted line) and derivative of trace distance $\sigma(t)$ (red dash-dot line), when the work qubit S_0 is initially prepared in the state $|1\rangle_0$. Moreover, (a)–(c) and (d)–(f) are related to the case of using fermionic and bosonic reservoirs, respectively. Besides, we set $T_1 = 0.5T_2$.

Assume that the interaction between the QATM S_{12} and the work qubit S_0 is conservative, namely, $[\sum_{i=0}^{2} \hat{H}_{S_i}, \hat{H}_{S_{12}S_0}] = 0$. This conservation implies that $\mathrm{Tr}\{\hat{H}_{S_{12}S_0}\dot{\hat{\rho}}_T(t)\} = 0$. In this regard, the stability condition of the total system $T = S12 \otimes S_0$ using the interaction Hamiltonian $\hat{H}_{S_{12}S_0}$ over time gives rise to

$$\dot{Q}_T(t) = \dot{Q}_{S_1}(t) + \dot{Q}_{S_2}(t) + \dot{Q}_{S_0}(t), \tag{29}$$

where $\dot{Q}_{S_i}(t) = -\mathrm{Tr}\{\hat{H}_i\dot{\hat{\rho}}_i(t)\}$ for $i = \{0, 1, 2\}$ represents the heat flux of each subsystem S_0, S_1, and S_2. Here, it is worth noting that the divisibility of heat flux is valid only when the total Hamiltonian in Eq. (1) is time-independent, with no external work exchanged between the total system T and the reservoirs R_1 and R_2. Indeed, this is according to the case of work exchange between the system and environment. Indeed, the strong coupling between them creates a strong correlation, making distinguishing between work and heat difficult. [56]. Using the quantum mutual information $I(t)$ between the thermal machine and the subsystem S_0, we find

$$-\dot{S}(\hat{\rho}_T(t)) = \dot{I}(t) - \dot{S}(\hat{\rho}_0(t)) - \dot{S}(\hat{\rho}_{12}(t)), \tag{30}$$

such that, combined with the Landauer bound in Eq. (27), we obtain our reformulation of the generalized Landauer lower bound for the subsystem S_0

$$\beta_v \dot{Q}_{S_0}(t) \geqslant \dot{I}(t) - \dot{S}(\hat{\rho}_{S_0}(t)) - \dot{S}(\hat{\rho}_{12}(t)) - \beta_v \sum_{m=1}^{2} \dot{Q}_{S_m}(t), \tag{31}$$

which describes a new, generalized, Landauer lower bound for the subsystem S_0 in non-Markovian dynamics. This expression captures the correlation between S_{12} and S_0, as well as the heat flux of each subsystem S_0, S_1, and S_2. Furthermore, one can observe that the conventional Landauer principle for S_0, namely $\beta_v \dot{Q}_{S_0}(t) \geqslant \Delta\dot{S}(\hat{\rho}_0(t))$, may be violated in comparison to the new Landauer limit.

To explore the relationship between the Landauer limit and non-Markovianity, one can utilize the derivative of the trace distance [48], defined as $\sigma(t) = \frac{d}{dt}D(\rho_0^A(t), \rho_0^B(t))$. The sign of $\sigma(t)$ can indicate the nature of the dynamics: $\sigma(t) < 0$ corresponds to a Markovian regime, while $\sigma(t) > 0$ indicates non-Markovian dynamics.

We now explore the manipulation of the new Landauer lower bound to non-Markovian dynamics through four examples. First, we consider the subsystem S_0 initialized in a superposition state $|\psi_A\rangle_0$ and coupled to the thermal machine S_{12} with two versions of reservoirs: bosonic and fermionic. Second, we analyze the case where the system S_0 is initially prepared in the state $|1_{S_0}\rangle$.

Figure 8 illustrates the behavior of the subsystem S_0, initially in the superposition state $|\psi_A\rangle_0$, under the influence of fermionic reservoirs [Figs. 8(a)–8(c)] and bosonic reservoirs [Figs. 8(d)–8(f)]. For the fermionic reservoirs, we examine the impact of temperature resonances between T_1 and T_2 on the heat flux $\beta_v \dot{Q}_{S_0}$, the exchanged entropy $\Delta\dot{S}_0 = \Delta\dot{S}(\hat{\rho}_0(t))$, the new lower Landauer bound (i.e., $\dot{I}(t) - \dot{S}(\hat{\rho}_0(t)) - \dot{S}(\hat{\rho}_{12}(t)) - \beta_v \sum_{m=1}^{2} \dot{Q}_{S_m}(t)$), and the derivative of the trace distance $\sigma(t)$.

Comparing the heat flux $\beta_v \dot{Q}_{S_0}$ with the exchanged entropy $\Delta\dot{S}_0$, we observe that when $\sigma(t) < 0$, the classical Landauer limit is satisfied, i.e., $\beta_v \dot{Q}_{S_0}(t) \geqslant \Delta\dot{S}(\hat{\rho}_0(t))$. Conversely, when the derivative of the trace distance is positive, $\sigma(t) > 0$, the classical Landauer bound is violated, meaning $\beta_v \dot{Q}_{S_0}(t) \leqslant \Delta\dot{S}(\hat{\rho}_0(t))$. Nonetheless, the new lower Landauer bound remains valid ($\beta_v \dot{Q}_{S_0}(t) \geqslant \dot{I}(t) - \dot{S}(\hat{\rho}_0(t)) - \dot{S}(\hat{\rho}_{12}(t)) - \beta_v \sum_{m=1}^{2} \dot{Q}_{S_m}(t)$) regardless of the sign of the derivative of the trace distance.

This analysis implies that the classical Landauer limit is highly dependent on the direction of information backflow between the work qubit S_0 and the reservoirs R_1 and R_2, mediated by the thermal machine S_{12}. It is important to note that the classical Landauer bound does not account for any properties of the thermal machine S_{12}. In contrast, the generalized lower Landauer bound incorporates the von Neumann entropies $\dot{S}(\hat{\rho}_0(t))$ and $\dot{S}(\hat{\rho}_{12}(t))$ of the system S_0 and the thermal machine S_{12}, respectively. Additionally, the mutual information $I(t)$ and the heat flux $\beta_v \sum_{m=1}^{2} \dot{Q}_{S_m}(t)$ play a crucial role. Thus, the new lower bound effectively captures the exchange of information between S_0 and S_{12}, as well as with R_1 and R_2.

Finally, in Fig. 9, we explore the dynamics of the proposed measures when S_0 is initially prepared in the state $|1\rangle_0$. Specifically, in Figs. 9(d)–9(f), we study the impact of the coupling strength between the system S_0 and the thermal machine S_{12} on the heat flux $\beta_v \dot{Q}_{S_0}$. We also calculate the exchanged entropy $\Delta\dot{S}_0 = \Delta\dot{S}(\hat{\rho}_0(t))$, the generalized Landauer lower bound (GLB) ($\dot{I}(t) - \dot{S}(\hat{\rho}_0(t)) - \dot{S}(\hat{\rho}_{12}(t)) - \beta_v \sum_{m=1}^{2} \dot{Q}_{S_m}(t)$), and the derivative of the trace distance $\sigma(t)$.

As observed in the top panels, the classical Landauer bound is violated due to the memory effects generated by the thermal machine, resulting in backflow between the system S_0 and the reservoirs R_1 and R_2. Notably, the new lower limit is consistently satisfied across all scenarios. This indicates that the memory effects induced by the thermal machine significantly influence the dynamics of the Landauer bound. While the classical Landauer bound may be violated, the new lower Landauer bound remains valid, highlighting the importance of accounting for correlations between the thermal machine and the work qubit S_0, as demonstrated in other investigations [53,54].

Through our work, we provide the minimal energy cost for erasing information under non-Markovian dynamics in the context of an autonomous quantum thermal machine. This opens new horizons for experimental discovery through our theoretical framework. Based on the experimental implementation outlined in Ref. [10], which utilizes a superconducting flux qubit and two quantum dots to realize a quantum autonomous thermal machine capable of generating a steady state or a quantum circuit as shown in Ref. [57], our framework can also be relied upon to develop quantum computing systems based on trapped ions, as examined in Ref. [58].

IV. CONCLUSION

In this work, we have investigated a theoretical model of a minimal two-qubit autonomous quantum thermal machine (QATM), denoted as S_{12}, coupled to a working qubit S_0. This thermal machine operates via excitation exchanges between its states, with each qubit—S_1 and S_2—coupled to its respective Markovian reservoirs R_1 and R_2. Our analysis revealed that the thermal machine plays a pivotal role in generating quantum coherence by inducing non-Markovian dynamics for the work qubit. We examined the dynamics of the trace distance for S_0 and analyzed the information exchange between S_{12} and S_0 using mutual information over time. Our results demonstrate a significant feedback mechanism, where information flows between the open system and the thermal machine, allowing the work qubit to exhibit non-Markovian dynamics and damped coherent oscillations through correlation exchanges with the thermal machine.

In the second part of this study, we focused on investigating both the conventional and new Landauer lower bounds within the context of non-Markovian dynamics across four different scenarios. First, we analyzed these bounds for S_0 initially prepared in a superposition state, coupled to the thermal machine S_{12} with bosonic and fermionic reservoirs. Second, we considered the case where S_0 is initially prepared in the state $|1\rangle$. Our findings indicate that the thermal machine qubits can be envisioned effectively as a unified entity at a virtual temperature T_v. We observed that the Landauer bound for the open system is fundamentally dependent on this virtual temperature.

We explored the relationship between non-Markovianity and the Landauer bound, demonstrating that the conventional Landauer bound can be violated due to the information backflow between the open system and the QATM due to finite size effects arising from the induced structured bath behavior of the joint working qubit-reservoir systems. To address this, we proposed a generalized lower Landauer bound that accounts for the minimum dissipation energy required to erase information, considering the return flow between the thermal machine and the open system. Our investigation comprehensively considers the influence of physical parameters embedded in the collective state of the interacting open system-thermal machine, in the presence of both bosonic and fermionic reservoirs. In particular, the non-Markovian character can be tuned by the S_0 and S_{12} coupling coefficients.

In addition to the fundamental significance of our results on the interplay of quantum coherence, structured baths, and non-Markovianity in the context of QATMs, considering the resource value of quantum coherence for quantum technologies, our results may serve towards energy-efficient quantum technology applications via autonomous production and storage of quantum coherence using thermal sources in compact qubit systems.

ACKNOWLEDGMENTS

A.K. acknowledges CNRST-Morocco support for this research within the Program “PhD-Associate Scholarship–PASS.” This work was supported by the Scientific and Technological Research Council of Türkiye (TÜBİTAK) under Project No. 123F150. Ö.E.M. thank TÜBİTAK for their support.

The authors declare that they have no conflict of interest.

DATA AVAILABILITY

No data statement is available.

[1] F. Tonner and G. Mahler, Autonomous quantum thermodynamic machines, Phys. Rev. E **72**, 066118 (2005).

[2] R. Kosloff, Quantum thermodynamics: A dynamical viewpoint, Entropy. **15**, 2100 (2013).

[3] J. Gemmer, M. Michel, and G. Mahler, *Quantum Thermodynamics: Emergence of Thermodynamic Behavior within Composite Quantum System*, Lecture Notes in Physics (Springer Berlin, Heidelberg, 2009).

[4] M. Carrega, L. Razzoli, P. A. Erdman, F. Cavaliere, G. Benenti, and M. Sassetti, Dissipation-induced collective advantage of a quantum thermal machine, AVS Quantum Sci. **6**, 025001 (2024).

[5] M. Drewsen and A. Imparato, Quantum duets working as autonomous thermal motors, Phys. Rev. E **100**, 042138 (2019).

[6] M. T. Mitchison, Quantum thermal absorption machines: Refrigerators, engines and clocks, Contemp. Phys. **60**, 164 (2019).

[7] Y. Khlifi, S. Seddik, and A. El Allati, Steady state entanglement behavior between two quantum refrigerators, Physica A **596**, 127199 (2022).

[8] M. H. B. A. Chakour, A. El Allati, and Y. Hassouni, Coupling of two autonomous quantum refrigerators: Collective and relative performances, Phys. Lett. A **451**, 128410 (2022).

[9] Y. Khlifi, A. El Allati, A. Salah, and Y. Hassouni, Evaluating the performance of a refrigerator by an external system using entanglement, Eur. Phys. J. D **75**, 195 (2021).

[10] J. B. Brask, G. Haack, N. Brunner, and M. Huber, Autonomous quantum thermal machine for generating steadystate entanglement, New J. Phys. **17**, 113029 (2015).

[11] A. Shah, S. Vinjanampathy, and B. Muralidharan, Classical information driven quantum dot thermal machines, Ann. Phys. (NY) **396**, 564 (2018).

[12] G. Manzano, R. Silva, and J. M. Parrondo, Autonomous thermal machine for amplification and control of energetic coherence, Phys. Rev. E **99**, 042135 (2019).

[13] I. Khait, J. Carrasquilla, and D. Segal, Optimal control of quantum thermal machines using machine learning, Phys. Rev. Res. **4**, L012029 (2022).

[14] J. Roßnagel, S. T. Dawkins, K. N. Tolazzi, O. Abah, E. Lutz, F. Schmidt-Kaler, and K. Singer, A single-atom heat engine, Sci. Adv. **352**, 325 (2016).

[15] J. Klatzow *et al.*, Experimental demonstration of quantum effects in the operation of microscopic heat engines, Phys. Rev. Lett. **122**, 110601 (2019).

[16] D. von Lindenfels, O. Grab, C. T. Schmiegelow, V. Kaushal, J. Schulz, M. T. Mitchison, J. Goold, F. Schmidt-Kaler, and U. G. Poschinger, Spin heat engine coupled to a harmonic-oscillator flywheel, Phys. Rev. Lett. **123**, 080602 (2019).

[17] N. Van Horne, D. Yum, T. Dutta, P. Hänggi, J. Gong, D. Poletti, and M. Mukherjee, Single-atom energy-conversion device with a quantum load, npj Quantum Inf. **6**, 37 (2020).

[18] M. Rasola and M. Möttönen, Autonomous quantum heat engine based on non-Markovian dynamics of an optomechanical Hamiltonian, Sci. Rep. **14**, 9448 (2024).

[19] A. El Allati, K. El Anouz, M. H. B. A. Chakour, and S. Al-Kuwari, Non-Markovian effects on the performance of a quantum Otto refrigerator, Phys. Lett. A **496**, 129316 (2024).

[20] K. Ptaszyński, Non-Markovian thermal operations boosting the performance of quantum heat engines, Phys. Rev. E **106**, 014114 (2022).

[21] P. A. Camati, J. F. G. Santos, and R. M. Serra, Employing non-Markovian effects to improve the performance of a quantum Otto refrigerator, Phys. Rev. A **102**, 012217 (2020).

[22] I. de Vega and D. Alonso, Dynamics of non-Markovian open quantum systems, Rev. Mod. Phys. **89**, 015001 (2017).

[23] M. H. B. A. Chakour, A. El Allati, and Y. Hassouni, On the coupling of three-level quantum refrigerators in the weak coupling limit, J. Phys. B: At. Mol. Opt. Phys. **57**, 105001 (2024).

[24] M. Popovic, B. Vacchini, and S. Campbell, Entropy production and correlations in a controlled non-Markovian setting, Phys. Rev. A **98**, 012130 (2018).

[25] Q. Zeng and J. Wang, New fluctuation theorems on Maxwell's demon, Sci. Adv. **7**, eabf1807 (2021).

[26] W.-M. Zhang, P. Y. Lo, H. N. Xiong, M. W.-Y. Tu, and F. Nori, General non-Markovian dynamics of open quantum systems, Phys. Rev. Lett. **109**, 170402 (2012).

[27] P. Abiuso and V. Giovannetti, Non-Markov enhancement of maximum power for quantum thermal machines, Phys. Rev. A **99**, 052106 (2019).

[28] Y. Aiache, C. Seida, K. El Anouz, and E. Al Allati, Non-Markovian enhancement of nonequilibrium quantum thermometry, Phys. Rev. E **110**, 024132 (2024).

[29] Y.-Y. Hsieh, Z.-Y. Su, and H.-S. Goan, Non-Markovianity, information backflow, and system-environment correlation for open-quantum-system processes, Phys. Rev. A **100**, 012120 (2019).

[30] A. M. Lacerda, M. J. Kewming, M. Brenes, C. Jackson, S. R. Clark, M. T. Mitchison, and J. Goold, Entropy production in the mesoscopic-leads formulation of quantum thermodynamics, Phys. Rev. E **110**, 014125 (2024).

[31] R. Landauer, Irreversibility and heat generation in the computing process, IBM J. Res. Dev. **5**, 183 (1961).

[32] S. Deffner and S. Campbell, *Quantum Thermodynamics: An Introduction to the Thermodynamics of Quantum Information* (Morgan & Claypool, 2019).

[33] S. Campbell, G. Guarnieri, M. Paternostro, and B. Vacchini, Nonequilibrium quantum bounds to Landauer's principle: Tightness and effectiveness, Phys. Rev. A **96**, 042109 (2017).

[34] H. Li, J. Zou, and B. Shao, Enhanced quantumness via non-Markovianity, Phys. Rev. A **104**, 052201 (2021).

[35] S. Lorenzo, R. McCloskey, F. Ciccarello, M. Paternostro, and G. M. Palma, Landauer's principle in multipartite open quantum system dynamics, Phys. Rev. Lett. **115**, 120403 (2015).

[36] N. Linden, S. Popescu, and P. Skrzypczyk, How small can thermal machines be? The smallest possible refrigerator, Phys. Rev. Lett. **105**, 130401 (2010).

[37] J.-Q. Li, L. Bai, and J.-Q. Liang, Entropic uncertainty relation under multiple bosonic reservoirs with filtering operator, Quantum Inf. Process. **17**, 206 (2018).

[38] G. G. Damas, R. J. de Assis, and N. G. de Almeida, Cooling with fermionic thermal reservoirs, Phys. Rev. E **107**, 034128 (2023).

[39] S. Lorenzo, F. Ciccarello, and G. M. Palma, Composite quantum collision models, Phys. Rev. A **96**, 032107 (2017).

[40] H.-P. Breuer and F. Petruccione, *The Theory of Open Quantum Systems* (Oxford University Press, 2002).

[41] A. R. Vargas, Open quantum systems and quantum information dynamics, Doctoral thesis, Universitaire Ulm, 2011.

[42] T. Baumgratz, M. Cramer, and M. B. Plenio, Quantifying coherence, Phys. Rev. Lett. **113**, 140401 (2014).

[43] Y. Aiache, K. El Anouz, N. Metwally, and A. El Allati, Dynamics of quantum coherence and nonlocality of a two-spin system in the chemical compass, Phys. Rev. E **109**, 034101 (2024).
[44] Y. Aiache, A. El Allati, and K. El Anouz, Harnessing coherence generation for precision single- and two-qubit quantum thermometry, Phys. Rev. A **110**, 032605 (2024).
[45] H. P. Breuer, E. M. Laine, J. Piilo, and B. Vacchini, *Colloquium:* Non-Markovian dynamics in open quantum systems, Rev. Mod. Phys. **88**, 021002 (2016).
[46] M. A. Nielsen and I. L. Chuang, *Quantum Computation and Quantum Information* (Cambridge University Press, 2010).
[47] N. Brunner, N. Linden, S. Popescu, and P. Skrzypczyk, Virtual qubits, virtual temperatures, and the foundations of thermodynamics, Phys. Rev. E **85**, 051117 (2012).
[48] S. Wißmann, H. P. Breuer, and B. Vacchini, Generalized trace-distance measure connecting quantum and classical non-Markovianity, Phys. Rev. A **92**, 042108 (2015).
[49] Z. X. Man, Y. J. Xia, and R. Lo Franco, Temperature effects on quantum non-Markovianity via collision models, Phys. Rev. A **97**, 062104 (2018).
[50] J. Goold, M. Paternostro, and K. Modi, Nonequilibrium quantum Landauer principle, Phys. Rev. Lett. **114**, 060602 (2015).
[51] Q. Zhang, Z. X. Man, and Y. J. Xia, Non-Markovianity and the Landauer principle in composite thermal environments, Phys. Rev. A **103**, 032201 (2021).
[52] D. Reeb and M. M. Wolf, An improved Landauer principle with finite-size corrections, New J. Phys. **16**, 103011 (2014).
[53] M. Pezzutto, M. Paternostro, and Y. Omar, Implications of non-Markovian quantum dynamics for the Landauer bound, New J. Phys. **18**, 123018 (2016).
[54] Z. X. Man, Y. J. Xia, and R. Lo Franco, Validity of the Landauer principle and quantum memory effects via collisional models, Phys. Rev. A **99**, 042106 (2019).
[55] G. Guarnieri, S. Campbell, J. Goold, S. Pigeon, B. Vacchini, and M. Paternostro, Full counting statistics approach to the quantum non-equilibrium Landauer bound, New J. Phys. **19**, 103038 (2017).
[56] P. Kumar, C. M. Webb, and C. A. Stafford, Work sum rule for open quantum systems, Phys. Rev. Lett. **133**, 070404 (2024).
[57] T. Yoshioka, H. Mukai, A. Tomonaga, S. Takada, Y. Okazaki, N. H. Kaneko, S. Nakamura, and J. S. Tsai, Active initialization experiment of a superconducting qubit using a quantum circuit refrigerator, Phys. Rev. Appl. **20**, 044077 (2023).
[58] P. Drmota *et al.*, Verifiable blind quantum computing with trapped ions and single photons, Phys. Rev. Lett. **132**, 150604 (2024).
[59] C. Jarzynski, Nonequilibrium equality for free energy differences, Phys. Rev. Lett. **78**, 2690 (1997).
[60] P. Talkner, E. Lutz, and P. Hänggi, Fluctuation theorems: Work is not an observable, Phys. Rev. E **75**, 050102 (2007).